Relationships between lineal fracture intensity and chemical composition in the Marcellus Shale, Appalachian Basin

Keithan G. Martin[1], Liaosha Song[2], Payam Kavousi[1], and Timothy R. Carr[1]

Abstract

Within mudrock reservoirs, brittle zones undergo failure during hydraulic stimulation, creating numerous artificial fractures which enable hydrocarbons to be liberated from the reservoir. Natural fractures in mudrock reduce the tensile strength of the host rock, creating planes of weaknesses that are hypothesized to be reactivated during hydraulic stimulation. Combined, brittleness and natural fractures contribute to creating more abundant and complex fracture networks during hydraulic stimulation. Research efforts toward quantifying rock brittleness have resulted in numerous mineral-/compositional-based indices, which are used during petrophysical analysis to predict zones most conducive to hydraulic stimulation. In contrast, investigations on the relationship between chemical composition and core-scale natural fractures are limited. For this study, we collected high-resolution energy-dispersive X-ray fluorescence (XRF) data, calibrated with a wave-dispersive XRF, from a Marcellus Shale core. Additionally, we characterized corescale natural fractures in terms of length, width, in-filling material or lack thereof, and orientation. Following the characterization, we transformed the natural fracture data into a continuous P10 (lineal fracture intensity) curve, expressed as the number of fractures per a one-half foot window. Using these data sets, we investigated the relationship between rock composition and natural fracture intensity. Regression analyses recorded positive relationships between natural fracture intensity and calcium, silicon/aluminum, and total organic carbon (TOC), and negative relationships with silicon and aluminum. Aluminum recorded the strongest (negative) relationship ($r^2 = 0.379$) with natural fracture intensity. To access the degree to which natural fractures can be predicted based on chemical composition, we applied a partial least-squares analysis, a multivariate method, and recorded an $r^2 = 0.56$. Our study illustrates that although numerous factors are responsible for natural fracture genesis, such fractures predictively concentrate in areas of similar chemical composition, largely in zones with low aluminum concentrations.

Introduction

The term "mudrock" will be used following Blatt et al. (1972), who uses mudrock as a broad term for fine- to very-fine-grained rocks (<62.5 μm in diameter) dominated (>50% of grains) by varying degrees of silt, mud, and clay concentration and include fissile and nonfissile rock. When further divided, fissile and nonfissile mudrocks are termed "shale" and "stone" respectively, and they are modified by the dominant grain size, such that a silt-rich, nonfissile mudrock would be termed a siltstone. Mudrock is a useful term for the Marcellus Shale specifically because it contains a spectrum of such fine- to very-fine-grained rocks.

Mudrock reservoirs are characterized by nanometer- to micrometer-size pores and nano- to microdarcy permeability (Loucks et al., 2012; Peng and Loucks, 2016; Milad and Slatt, 2018). Such reservoir characteristics significantly impede the ability for hydrocarbons to flow through the formation into the borehole. Advances in hydraulic fracturing technology over the last decade have allowed for the exploitation of hydrocarbons from mudrock reservoirs by generating artificial fractures, which create permeability for liquid and gaseous hydrocarbons to flow through rock into the borehole.

Rock brittleness and ductility are key variables in determining a rock's conduciveness to hydraulic stimulation. A ductile rock will absorb a high amount of energy before fracturing, whereas a brittle rock will fail and more readily form fractures (Zhang et al., 2015). Research efforts have attempted to quantify brittleness through mechanical testing, mineral content, elastic parameters, and sedimentary characteristics (Chang et al., 2006). Within silica-rich Woodford Shale intervals, anisotropic features, such as laminations and bedding, were charac-

[1]West Virginia University, Department of Geology and Geography, Morgantown, West Virginia 26506, USA. E-mail: kgm0002@mix.wvu.edu; pkavousi@mix.wvu.edu; tim.carr@mail.wvu.edu.

[2]Formerly West Virginia University, Department of Geology and Geography, Morgantown, West Virginia 26506, USA; presently California State University, Bakersfield, Department of Geological Sciences, Bakersfield, California 93311, USA. E-mail: liaoshasong@gmail.com.

Manuscript received by the Editor 26 November 2018; revised manuscript received 31 January 2019; published ahead of production 11 June 2019; published online 9 September 2019. This paper appears in *Interpretation*, Vol. 7, No. 4 (November 2019); p. SJ33–SJ43, 8 FIGS.

http://dx.doi.org/10.1190/INT-2018-0221.1.

terized by lower resistance to fracture and tensile strength, indicating that anisotropic features may contribute to the fracability of a unit (Molinares et al., 2017). In addition to anisotropic features, mineral composition plays a large role in the overall brittleness of a rock (Jarvie et al. 2007; Slatt and Abousleiman, 2011). It is now widely held that enrichment of silica contributes to brittleness, whereas an enrichment of total organic carbon (TOC) and clay increase ductility. Jarvie et al. (2007) conclude that silica was the only contributor to brittleness, whereas clay and carbonate increased ductility. Wang and Gale (2009) find similar results, but they differentiate between dolomite and calcite, claiming that although calcite does contribute to ductility, dolomite has a brittle behavior. More recently, Jin et al. (2014) conclude that quartz, feldspars, brittle mica, and carbonate all contribute to brittleness.

Within unconventional mudrock exploration, units with high TOC are desirable. The fact that TOC contributes to ductility complicates locating zones that are organic rich and also conducive to artificial stimulation. Using Passey's method to derive TOC and the brittleness equation of Wang and Gale, (2009) and Verma et al. (2016) confirm that TOC has a negative relationship with brittleness.

In addition to rock brittleness, natural fractures play a significant role in the effectiveness of hydraulic stimulation (Olson et al., 2001; Rijken, 2005; Gale et al., 2007). It has been hypothesized that natural fractures form as a result of potentially one or a number of mechanisms, including tectonic events that cause local and regional stress changes, uplift, differential compaction, strain from the accommodation of large structures, and catagenesis (Neuzil and Pollock, 1983; Jowett, 1987; Price, 1997; Gale et al., 2007; Engelder et al., 2009; Rodrigues et al., 2009; Milad and Slatt, 2018). Natural fractures, either mineralized (sealed) or open, can reactivate during hydraulic stimulation and create more complex fracture networks than could be achieved with a single hydraulic fracture (Gale et al., 2007). This is largely because natural fractures, in some cases, can act as a plane of weakness. Within the Barnett Shale, Wang and Gale (2009) observed that calcite-filled fractures were half as strong as an unbroken rock due to the lack of chemical bonding between the calcite in-filling the natural fracture and the fractured host rock. In addition to academic studies, empirical observations made during analysis of the Marcellus Shale core show that breakages/fractures along mineralized fractures and anisotropic planes occur at a rate much higher than a fractureless or more massive cored interval.

Brittleness and natural fractures play a role in the effectiveness of hydraulic stimulation. Although knowledge of the relationship between chemical composition and rock brittleness have advanced, studies addressing the relationship between chemical composition and core-scale natural fracture presence are lacking. To address this shortcoming, we use high-resolution X-ray fluorescence data and detailed natural fracture data collected from the study well core to define the relationship between chemical composition and natural (open and mineralized) fractures. Questions that will be addressed include

1) Do natural fractures preferentially concentrate in rock of certain chemical composition in a statistically meaningful way?
2) If so, what chemical composition is most likely to have a positive or negative relationship with the natural fracture presence?
3) Are the relationships strong enough for natural fracture prediction based on chemical composition?
4) If so, can existing mineral-based brittleness indexes also be used for natural fracture prediction?
5) If not, can findings be used to create a chemical-based natural fracture index for natural fracture prediction?

Middle Devonian stratigraphy of the Appalachian Basin

The Marcellus Shale is divided into in three members, namely the Oatka Creek, Cherry Valley or Purcell Limestone, and the Union Springs members (Lash and Engelder, 2011). The Marcellus Shale is overlain by the Skaneateles Formation and overlies the Onondaga Limestone.

The Union Springs Member, informally referred to as the lower Marcellus, is thinnest in western New York and thickens to the east and southeast, reaching a thickness exceeding 160 ft (49 m) in northeastern Pennsylvanian (Lash and Engelder, 2011). This member is highly organic, calcareous, and it is characterized as a dark-gray to black mudrock containing skeletal material (Sageman et al., 2003). The lower portion of the Union Springs Member records a particularly high gamma-ray response, reaching upwards of 650 API units. This interval is characterized by a decrease in clay content and a significant increase in quartz, pyrite, and TOC (Lash and Engelder, 2011). The Union Springs Member overlies the Onondoga Limestone, which is interpreted as an unconformity, but it can be found to be conformable in Pennsylvania, western New York, and Ohio and Maryland (Lash and Engelder, 2011). The Cherry Valley Member, informally referred to as the "middle Marcellus" and is a stratigraphically equivalent unit of the Purcell Limestone of Pennsylvania and West Virginia, overlies the Union Spring Member (Lash and Engelder, 2011). This unit is a medium-gray packstone chiefly composed of significant skeletal debris, and it contains intervals of mudrock and siltstone. The thickness of the member ranges from tens of feet in New York to well over 100 ft (30 m) in northeastern Pennsylvania. Overlying the Cherry Valley Member is the Oatka Creek Formation, informally referred to as the upper Marcellus. This unit is defined as a medium to dark-gray mudstone with an underlying interval of black organic-rich mudstone.

Study area and general character of the core

A 105 ft Marcellus Shale core, labeled study well no. 1, located in the south-central portion of the Appalachian Basin was evaluated for this study (Figure 1). A composite of the general character of the Marcellus Shale core is displayed in Figure 2. Observations made during core analysis in conjunction with remarks made by Core Laboratories will be outlined starting with the deepest stratigraphic unit.

The Onondaga Limestone is a medium-gray, heavily bioturbated, laminated, microcrystalline limestone interbedded with silty, calcarerous shale. The interbedded silty shale intervals contain brachiopods, styliolinids, and other disarticulated fossil fragments. Multiple thin volcanic ash beds are distributed throughout most Onondaga intervals. The lower Marcellus Shale is a grayish black to dark gray, massively bedded, calcareous, organic-rich silty shale. This interval contains significant pyritic content: laminations, concretions, and nodules. As this interval comes in closer contact with the underlying Onondaga Limestone, the silty shale becomes more calcareous and the natural fracture concentration increases, most of which are infilled with calcite. Moving up the interval, the upper Marcellus Shale is massive to laminated, and it is less calcareous than its lower counterpart, although calcareous concretions are still present in small numbers. Pyrite nodules and pyritized fossils become more prevalent further up the interval and the clay content is moderate. Moderate to high organic content continues through most of the Marcellus Shale interval. The lower Manhantango Formation is a medium- to dark-gray, bioturbated, silty mudstone to calcareous mudstone. Gastropods and brachiopods make up the bulk of the skeletal debris, with crinoids, coral, and styliolinids making up the remaining fraction. Burrows are common, with many being infilled with pyrite. The upper Manhantango most notably differs through the loss of calcareous intervals, trace fossil presence, and pyrite infill, laminations, and nodules.

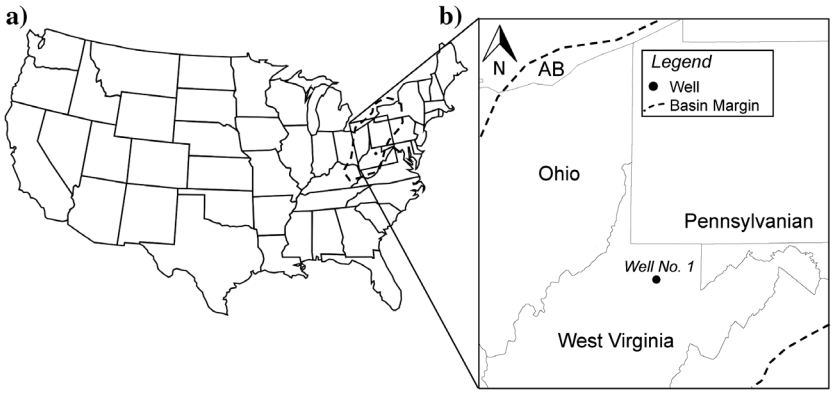

Figure 1. (a) United States map displaying the location of the study well no. 1 within the Appalachian Basin. The Appalachian Basin, AB, is represented by the dashed polygon. The skewed rectangle represents the study area for this research. (b) An expanded view of the study area, highlighting the location of study well no. 1 in West Virginia. The dashed lines represent the margins of the Appalachian Basin.

Brittleness

Brittleness is defined as the measurement of the ability of rock to fail (crack or fracture), representing a complex interplay among the rock strength, lithology, texture, effective stress, temperature, fluid time, diagenesis, and TOC (Handin and Hager, 1957; Davis and Reynold, 1996; Wells, 2004; Wang and Gale, 2009). Rock brittleness is a key variable in determining a rock's conduciveness to hydraulic stimulation. Brittleness and its inverse, ductility, are derived rock properties that are widely used to describe the deformation of a rock under stress. When brittleness is calculated over numerous feet of rock, it is often referred to as a brittleness index.

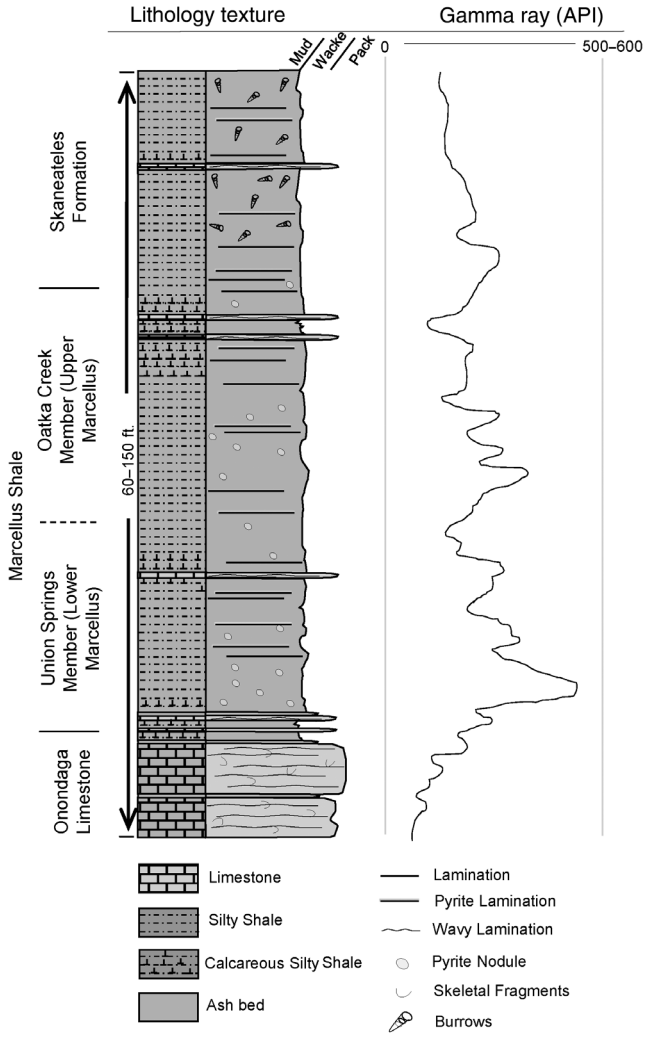

Figure 2. Composite of the general characteristics of core from study well nos. 1 and 2 displaying the formations, lithology, texture profile, and gamma-ray signature.

During hydraulic stimulation, a high brittleness index is most likely to indicate the following three positive characteristics: efficient fracture initiation and propagation, increased fracture complexity, and resistance to proppant embedment (Kias et al., 2015). A ductile rock will absorb a high amount of energy before fracturing, whereas a brittle rock will fail under a lower amount of energy and will form fractures (Rickman et al. 2008; Kundert and Mullen, 2009; Zhang et al., 2015). In the case that sufficient energy is applied to a ductile rock and is subsequently fractured and the newly created fractures are held open by proppants, the ductile rock will "heal" the fractures by embedding the proppants, compromising permeability.

Mineral composition plays a large role in the overall brittleness of a rock (Jarvie et al., 2007; Slatt and Abousleiman, 2011). It is widely held that brittleness has a positive relationship with increasing the quartz content, whereas ductility has a positive relationship with increasing clay minerals and TOC (Wang and Gale, 2009; Abouelresh and Slatt, 2012; Jin et al., 2014). Initially, Jarvie et al. (2007) find that incorporating quartz as a brittle material and calcite and clay minerals as ductile materials provided a more comprehensive brittleness equation and is expressed as

$$\mathrm{BI} = \mathrm{Q}/(\mathrm{Q} + \mathrm{C} + \mathrm{CL}), \tag{1}$$

where BI is the brittleness index, Q denotes quartz, C denotes carbonate — calcite and dolomite, and CL stands for clay.

This brittleness equation implies that quartz is the only mineral contributing to brittleness. Wang and Gale (2009) modify this equation by incorporated ideas from Wells (2004), who determine that the presence of dolomite tends to increase the brittleness of mudrock because dolomite is more brittle than limestone and organic matter tends to increase ductility. The modified equation is defined as

$$\mathrm{BI} = \mathrm{Q} + \mathrm{Dol}/(\mathrm{Q} + \mathrm{Dol} + \mathrm{Lm} + \mathrm{Cl} + \mathrm{TOC}), \tag{2}$$

where Dol denotes dolomite, Lm stands for limestone, and TOC is the total organic carbon.

In addition to defining quartz and dolomite as brittle minerals, Jin et al. (2014) observe that silicate minerals, including feldspar and mica (if the X ion within the chemical expression of mica, $X_2Y_{4\text{-}6}Z_8O_20$ (OH, F_4), is Ca), are considered brittle minerals. It was also concluded that carbonate other than dolomite, such as calcite, were more brittle than clay minerals. Jin et al. (2014) use these conclusions in a new expression of brittleness:

$$\mathrm{BI}: (W_{\mathrm{qtz}} + W_{\mathrm{carb}})/W_{\mathrm{total}}, \tag{3}$$

where W_{qtz} is the weight of quartz, feldspar, and mica, W_{carb} is the weight of carbonates, and W_{total} is the total mineral weight.

Geochemical proxies

Major elements, which make up multiple weight percent of a rocks composition, have a large effect on a rock's behavior under stress and, for this reason, will be the focal point of this study (Jarvie et al., 2007; Slatt and Abousleiman, 2011). These elements and element ratios include Si, Al, Ca, and Si/Al. Aluminum is found in common clay minerals such as smectite, illite, and chlorite. For most sedimentary deposits, Al represents the aluminosilicate fraction of the sediments and has little disposition for movement during diagenesis (Calvert and Pedersen, 1993; Morford and Emerson, 1999; Piper and Perkins, 2004; Tribovillard et al., 2006). Due to these characteristics, it is generally considered as the main proxy for clay minerals (Sageman and Lyons, 2003). Although Al, as well as titanium, is almost exclusively a product of crustal weathering, Si can be continentally and biogenically derived (Pearce and Jarvis, 1992; Pearce et al., 1999; Sageman and Lyons, 2003). To differentiate between detrital quartz and autogenic quartz, a ratio between Si and Al is often used. This ratio operates off the principle that as detrital Al decreases or increases, detrital Si should also decrease or increase. A decrease in Al with an increase in Si indicates an increase in autogenic influence as ratio increases. Autogenic silica enrichment takes place when dissolved silica is taken from the water column by diatoms and radiolarians to produce their siliceous skeletal frame (Prothero and Schwab, 1996). Opaline quartz is unstable and commonly undergoes a phase transition into a more stable form. Upon transition, silica precipitates into a more stable form and often becomes associated with organic matter, which ultimately ends up as an organic-rich gas reservoir upon burial maturation (Blood et al., 2013). Additionally, as silica is precipitated, it permeates the clay fabric of mudstones, ultimately increasing the overall brittleness of a rock unit (Blood et al., 2013). Calcium is incorporated into calcite, dolomite, and aragonite. Carbonate rocks are limestone and dolomite composed of the minerals calcite ($CaCO_3$) and dolomite ($CaMg(Co_3)_2$) (Flgel, 2004). Particles that make up carbonate rock either precipitate directly from the seawater or are biologically formed from calcified microbes, calcareous algae, and the articulated or disarticulated skeletons of marine organism (James and Jones, 2016).

Methods

Geochemical data used in this study were collected by a handheld X-ray fluorescence (HHXRF) analyzer. The HHXRF analyzers provide a nondestructive method for collecting elemental concentrations at centimeter resolution with detection limits in the tens of parts per million ranges (Lash and Blood, 2014). When investigating numerous cores over hundreds of feet, the use of an HHXRF, compared to other laboratory techniques such as wave-dispersive X-ray fluorescence (WDXRF) and inductively coupled plasma mass spectrometry analysis, is significantly more cost effective and time

efficient. In addition, more recent advances in the HHXRF technology have increased the analytical quality of the data. This has provoked a wider application of this technology in solving geologic problems, including chemostratigraphic studies of mudrock (Rothwell and Rack, 2006; Lowemark et al., 2011; Mainali, 2011; Rowe et al., 2012; Lash and Blood, 2014).

Core from study well no. 1 was analyzed with the Olympus Innov-X DELTA Premium Handheld XRF Analyzer, equipped with a 40 kV tube and large area silicon drift detector. With Delta's two-beam setting, a high (40 kV) and low (15 kV) beam is used to increase the resolution of the major and trace elements. With the Olympus Innov-X DELTA Premium Handheld XRF Analyzer specifically, Young et al. (2016) find that data obtained through the HHXRF analyzer is comparable to bench-top XRF analysis for geologically important elements, but it loses reliability with magnesium and any element lighter than magnesium. Similar findings were obtained in this study. The HHXRF data quality was controlled by scanning internal reference samples of the Marcellus Shale to monitor instrument drift before each data collection session. To address how quantitative the data collect were, 15 sample points taken throughout the core interval of study well no. 1 were scanned and subsequently plugged using a drill press. These core plugs were crushed, powdered, fused into a glass disk, and analyzed using a Thermo ARL Perform'X. The Thermo ARL Perform'X, a WDXRF, is a sequential X-ray fluorescence spectrometer capable of reading a suite of 44 elements. The WDXRF yields data that are three to five more precise than most HHXRFs, and it was calibrated with more than 70 certified reference materials. A regression analysis of data collected from the HHXRF and WDXRF recorded the following R^2 values for Si, Ca, and Al, respectively, 0.908, 0.986, and 0.962 (Figure 3a–3c). Using the slope-intercept equation from the regression analyses, the HHXRF data were calibrated to the WDXRF data.

TOC data were available for both study wells, as well as core spectral gamma-ray data. Spectral gamma-ray records concentrations of thorium, potassium, and uranium. Relationships have been defined to predict TOC from uranium content collected from spectral gamma ray (Bell et al., 1940; Schmoker, 1981; Zelt, 1985; Luning and Kolonic, 2003). A regression analysis between TOC and uranium (from spectral gamma) in study well no. 1 recorded an R^2 value of 0.843. To create a continuous TOC curve, the slope-intercept equation from the regression analysis was used to calibrate the uranium values to TOC (Figure 3d).

To access the relationship between natural fractures and chemical composition, two regression-based methods were used. First, a standard bivariate analysis was used to assess the relationship between the continuous variables. A "simple moving average" smoothing model was applied to the natural fracture data and elemental data. Both data were smoothed over a 1 ft moving window. This upscaling process created a continuous lineal fracture intensity (P10) curve. The P10 curve, expressed as the number of fractures per foot, was derived to enable regression analyses between P10 and Si, Al, Ca, Si/Al, and TOC. A partial least-squares analysis was conducted to evaluate the capabilities of Al, Si, Ca, TOC, and Si/Al to predict the natural fracture presence. This regression analysis method combines regression modeling, data structure simplification, and correlation analysis between two groups of variables, which maximizes the correlativity between independent and dependent variable, and it improves the correlation analysis accuracy of the model (Huang, 2018).

Results

Fracture characterization

Natural fracture data were collected from the study well nos. 1 and 2 core intervals. Fractures within the evaluated core intervals include drilling-induced, mineralized, and open fractures. Criteria used for differentiating artificial or drilling-induced fractures from open, natural fractures included the presence of slickensides, any signs of mineralization on the fracture surface, and rubble zones. Fractures evaluated include bedding-parallel fractures, vertical to subvertical fractures, concretion-related fractures, and compacted fractures (Figure 4). Calcite is the dominate infilling mineral of the mineralized fractures, although pyrite and dolomite were scarcely present. Within the 105 ft core from study

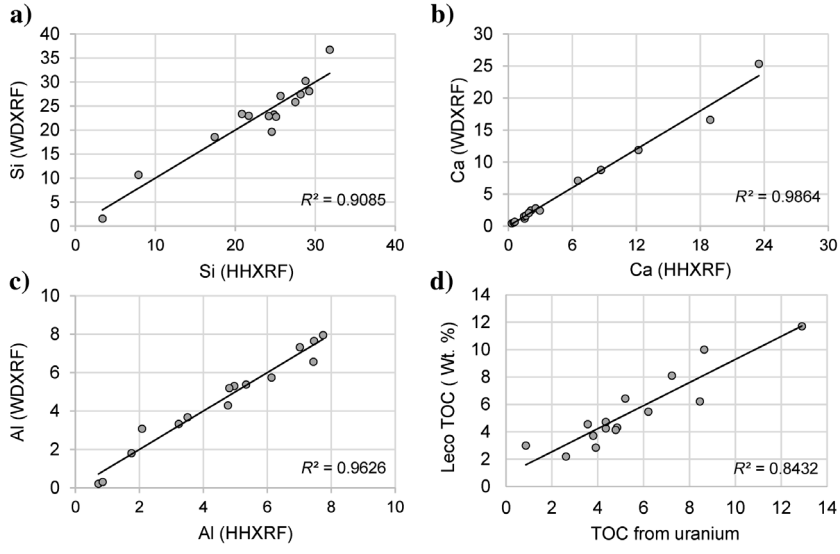

Figure 3. (a-c) Crossplot of elemental data (Si, Ca, and Al) collected from WDXRF and HHXRF with R^2 values on display. (d) Crossplot of TOC and uranium with the R^2 value on display.

well no. 1, the numbers of mineralized and open fractures observed were 319 and 204, respectively, with the sum of the natural fractures equaling 523. Figure 5 integrates the natural fracture data and elemental curves in a log view. Open, mineralized, and natural (total) fractures are shown as the natural fracture intensities per half-foot window. Relatively large smoothing windows coarsen and decrease the resolution of the data; therefore, smaller smoothing windows are desired. The half-foot window was found to be the optimal smoothing interval because it was the smallest interval that sufficiently smoothed the data to enable comparability with the geochemical data.

The foundation of this study comes from the HHXRF response of the Marcellus Shale core. To illustrate the relationships derived in this study, it is useful to see the direct elemental response to fracture presence (Figure 6). Figure 6 displays a core photo, CT scan, and standardized elemental values of Si, Si/Al, Al, and Ca, as well as TOC. Figure 6a is an example of a core interval that contains drilling-induced fractures along laminated surfaces but contains no natural fractures. As seen in the standardized elemental response, Al and silica are enriched throughout this core interval. Next, in Figure 6b, there is a naturally fractured zone between 7526.8 and 7527.2 ft. This corresponds with a significant depletion of Si and Al, whereas Si/Al, an autogenic quartz proxy, is enriched. Figure 6c displays two zones of natural fractures. First, between 7541.6 and 7542.1 ft, there are horizontal natural fractures that correspond with a significant depletion of Si and Al and an enrichment in Si/Al. The second set of fractures is located within a calcitic zone between 7542.6 and 7543.2. The corresponding elemental response includes a very significant depletion of Si and Al and a large enrichment of Ca.

Regression-based analyses

From the bivariate analysis, Si recorded a weak negative relationship ($r^2 = 0.159$) with fracture intensity, whereas TOC recorded a very weak positive relationship with fracture intensity ($r^2 = 0.047$). Ca and Si/Al recorded weak positive relationships with fracture intensity, with r^2 values of 0.118 and 0.283, respectively. Al recorded the strongest (negative) relationship with fracture intensity, with an r^2 value of 0.379. The partial least-squares analysis, which integrated all variables to predict P10, recorded an r^2 value of 0.5624, indicating that natural fractures predictively concentrate in compositionally similar intervals (Figures 7 and 8).

Discussion

Natural fractures form as a result of potentially one or a number of mechanisms, including tectonic events that cause local and regional stress changes, uplift, differential compaction, strain from the accommodation of large structures, and catagensis (Neuzil and Pollock, 1983; Jowett, 1987; Gale et al., 2007; Engelder et al., 2009; Rodrigues et al., 2009). Although such variables are often difficult to quantify, numerous methods can be used to measure, model, and predict chemical

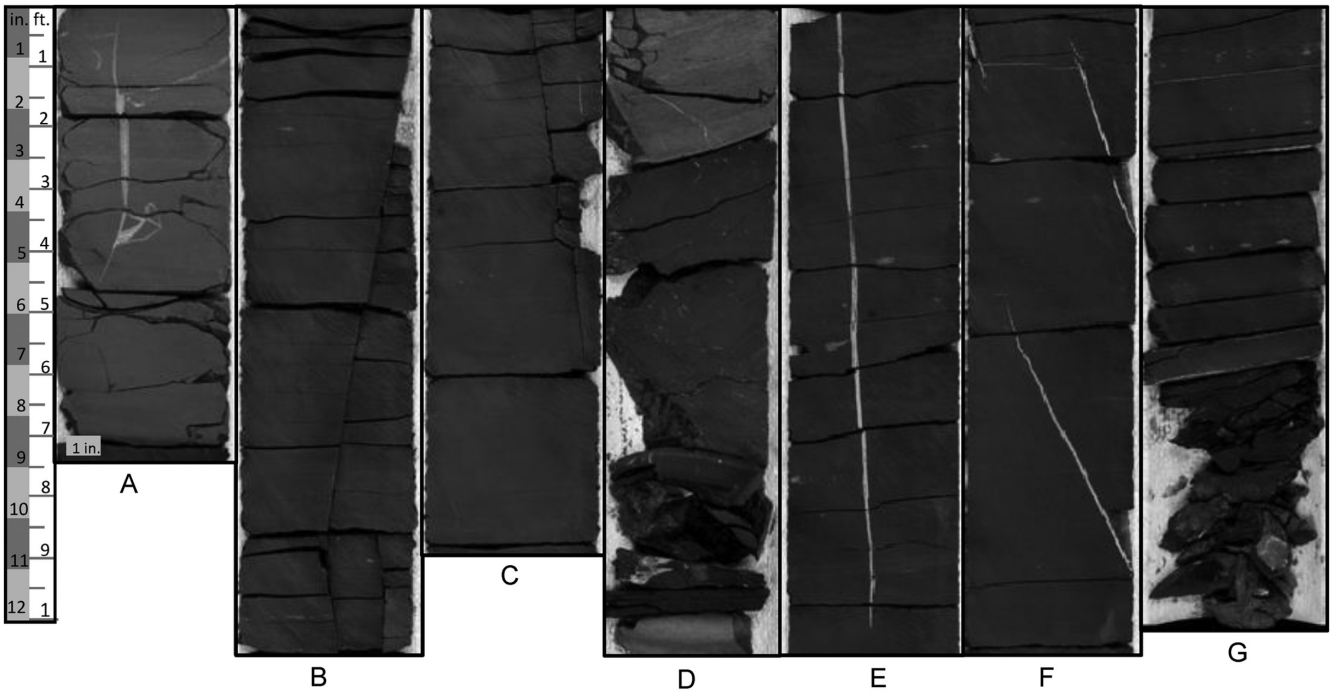

Figure 4. Display of the variety of natural and open fractures defined in this study. All mineralized fractures are infilled with calcite. A — Semicompacted vertical mineralized fracture, B and C — Vertical to subvertical open fracture, D — Subvertical to bedding parallel open fractures, E — Vertical mineralized fractures, F — Subvertical mineralized fractures, and G — Bedding parallel mineralized and open fractures.

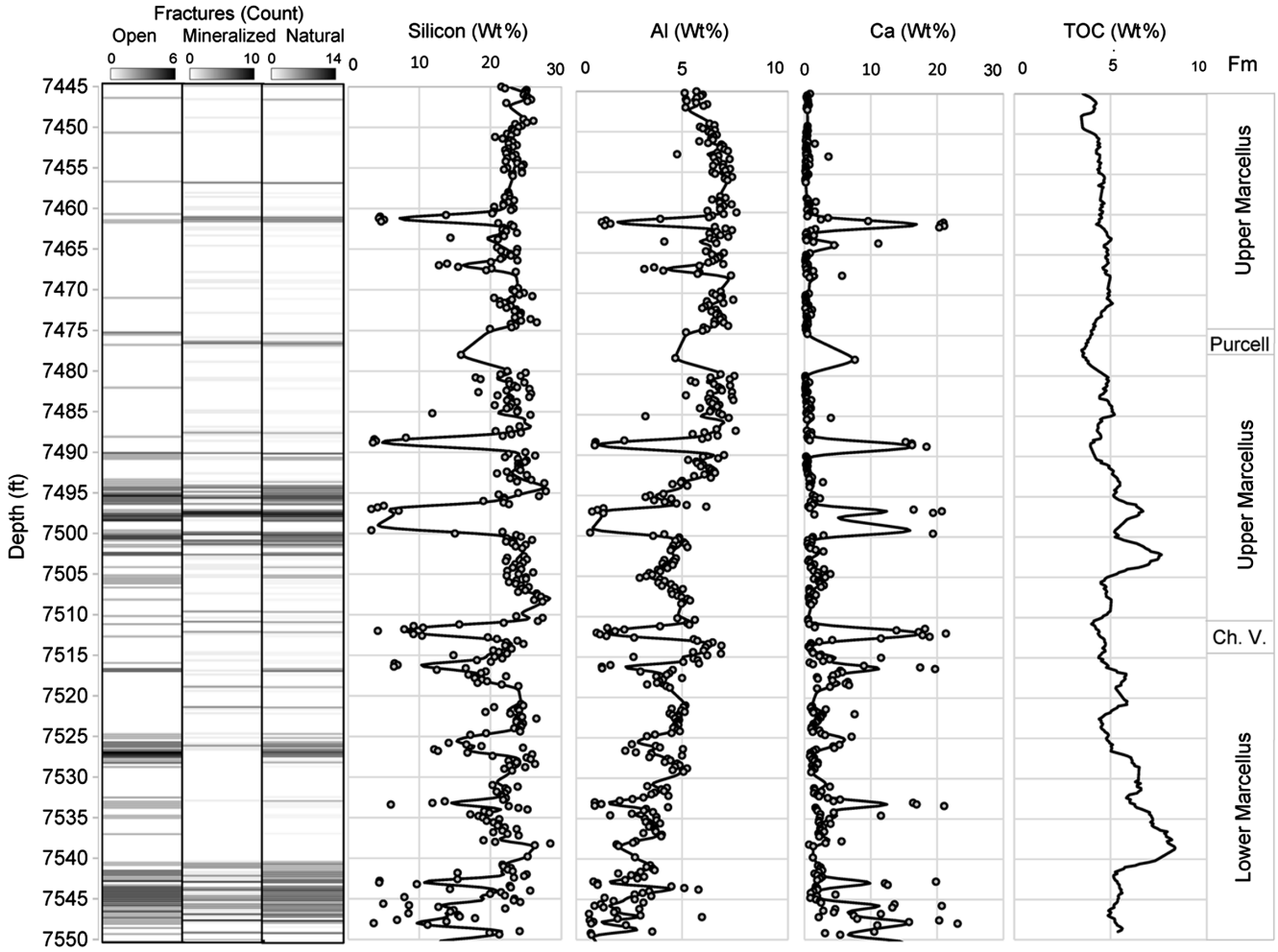

Figure 5. Starting on the left, fracture intensity of open, mineralized, and natural (total) fractures are displayed relative to depth. The color gradient indicates intervals that have a higher frequency of fractures within a half-foot window, with white representing low to no fractures and the increasing intensity becoming progressively darker. Si, Al, and Ca are displayed as individual data points and a smoothed curve to highlight gross trends. Formations (Fm) are located on the far right, with "Ch. V." abbreviating Cherry Valley.

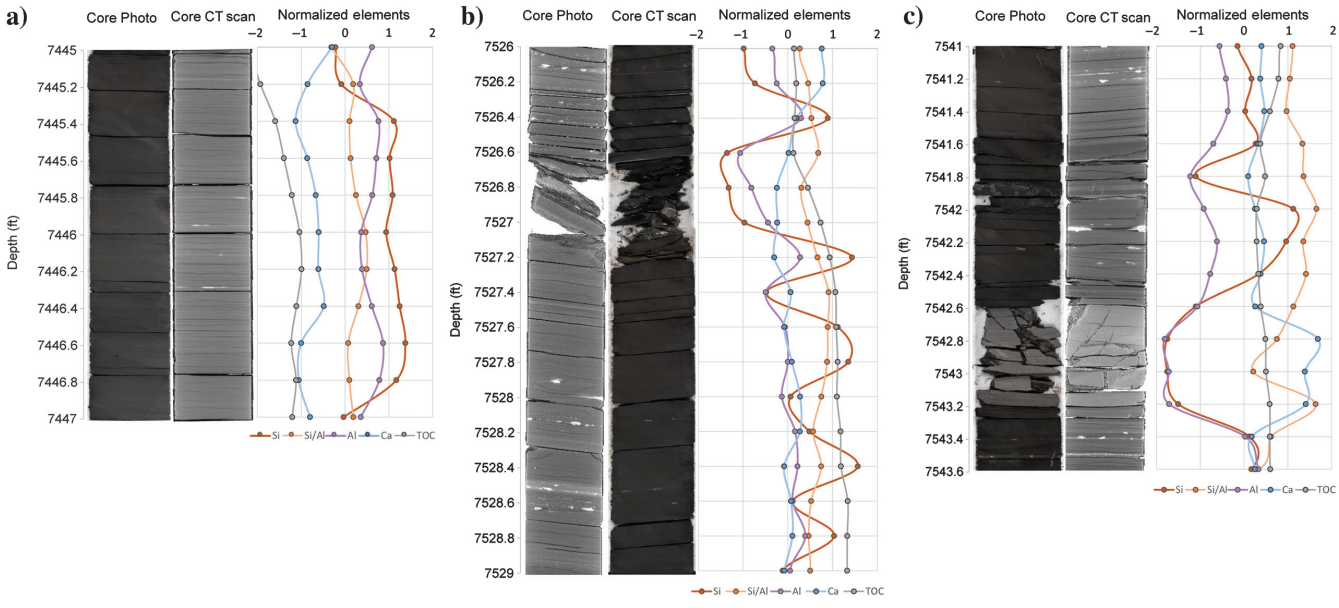

Figure 6. Display of three core intervals, including core photos, core CT scans, and normalized elemental concentrations (unitless).

composition of rock units. Thus, this study attempts to answer the degree to which natural fractures preferentially concentrate in compositionally similar rock intervals.

Results from the statistical analyses show that Ca, TOC, and Si/Al have moderate positive relationships with P10, whereas Si and Al record negative relationships with P10. Enrichment in Ca is largely responding to calcite nodules and calcitic zones (Figure 6c). A conclusion that could be drawn from the weak positive correlation between Ca and P10 is that the material infilling mineralized fractures, which is overwhelmingly calcite, could be causing the enrichment of Ca. In this case, the enrichment could potentially be responding to the calcite infill and not the composition of the rock matrix. There are two reasons that an enrichment in Ca is more than a response to calcite infilling the natural fractures, and an enrichment in Ca is in fact a response to the host rock. First, the HHXRF data were collected in evenly spaced increments down the center of the core to avoid sampling bias. Mineralized fractures would have to be consistently located within the center of the core for the calcite enrichment to source from mineralized fractures, which wasn't a characteristic found during core evaluation. Second, in general, open and mineralized fractures have a positive relationship with each other. Zones of high fracture presence with open, nonmineralized fractures often coincide with the high fracture presence of mineralized fractures (Figure 5). This provides evidence that Ca enrichment within highly fractured zones is a response to the overall chemical composition of rock, as opposed to the calcite infilling the natural fracture.

The TOC has a complex relationship with natural fracture presence. As made clear by Wang and Gale (2009) and others, TOC contributes to ductility, although TOC displayed a weak positive relationship with increasing fracture intensity (Figure 6b). As stated previously, autogenic silica (approximated by Si/Al) enrichment takes place when dissolved silica is taken from the water column by diatoms and radiolarians to produce their opaline skeletal frame. Upon dissolution, silica precipitates into a more stable for and often associates with organic matter (Blood et al., 2013). It was found by Blood et al. (2013) that, within organic-rich reservoirs, autogenic quartz provides a high-modulus medium, ultimately increasing the brittleness of the reservoir rock. This would indicate when an increase in TOC won't behave in a ductile manner contingent on the coincidence with elevated levels of Si/Al.

Within the brittleness indices discussed above (Jarvie et al., 2007; Wang and Gale, 2009; Jin et al., 2014), silica is claimed to contribute to the overall brittleness of a unit, whereas Al is claimed to contribute to the overall ductility of a unit. The hypothesis that brittle zones contain higher fracture intensity appears to be straightforward, although results from the statistical analyses among P10, and Si and Al demonstrate a weak to moderate negative relationship, respectively. Al has the strongest (negative) relationship with P10, recording an R^2 value of 0.379. Regression analysis between Si and Al records

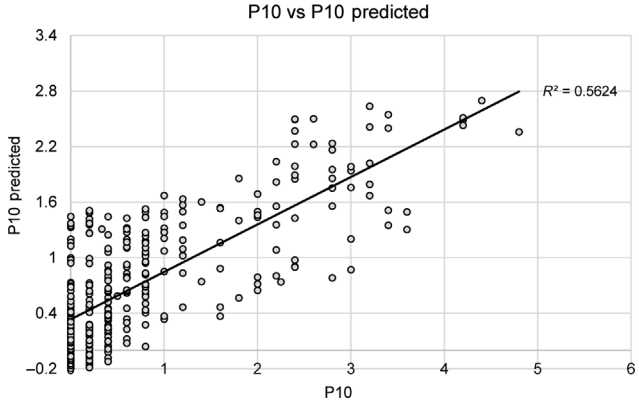

Figure 7. Crossplot displaying P10 predicted from the partial least-squares analysis on the y-axis and P10, which represents the natural fracture intensity derived from core evaluation, on the x-axis.

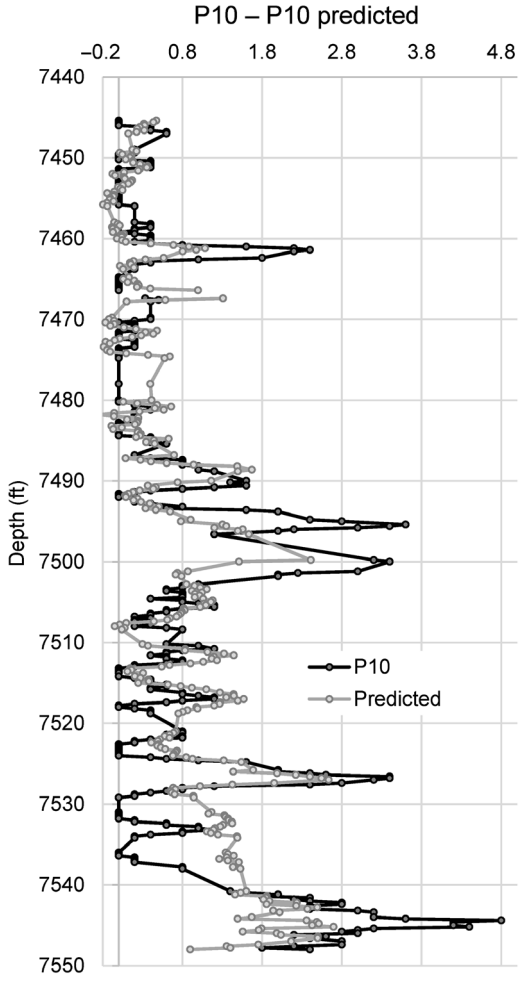

Figure 8. Log view showing the correlation between P10 predicted from the plot, the partial least-square analysis in light gray, and P10, which represents the natural fracture intensity derived from core evaluation, in black.

an R^2 value of 0.562. Due to the Al having the strongest relationship with P10, Si's negative relationship with P10 is most likely resulting from its covariation with Al, which is demonstrated by Si/Al having a positive relationship ($R^2 = 0.283$) with P10. This indicates that existing brittleness indices cannot predict natural fracture presence within the Marcellus Shale.

Conclusion

Prior to this study, the relationship between chemical composition and natural fracture intensity within the Marcellus Shale was underdeveloped. In addition, the applicability of existing brittleness indices for predicting areas of high natural fracture intensity was also unclear. The following were concluded from this investigation:

1) Existing brittleness indexes are not optimal for predicting natural fracture presence in the Marcellus Shale.
2) Ca has a strong positive relationship with increasing fracture intensity.
3) Al has a strong negative relationship with increasing fracture intensity.
4) Si and TOC have a moderate-to-weak relationship with natural fracture intensity.
5) Natural fractures preferentially concentrate in host rocks of similar chemical composition.

Future work

To reinforce the relationship between the natural fractures and chemical composition found in this study, fracture characterization of core and collection of XRF data on additional core is needed. HHXRFs provide high-resolution and dense data sets that can be used to derive statistically valid relationships. Additional work could attempt to correlate hardness, approximated by a rebound hammer, with the chemical composition collected from a HHXRF.

Acknowledgments

This research was funded through the U.S. Department of Energy — National Energy Technology Lab as part of their Marcellus Shale Energy and Environmental Laboratory (MSEEL) project (DOE Award No.: DE-FE0024297).

Data and materials availability

Data associated with this research are confidential and cannot be released.

References

Abouelresh, M., and R. M. Slatt, 2012, Lithofacies and sequence stratigraphy of the Barnett Shale in east-central Forth Worth basin, Texas: AAPG Bulletin, **96**, no. 1, 1–22, doi: 10.1306/04261110116.

Bell, K. G., C. Goodman, and W. L. Whitehead, 1940, Radioactive of sedimentary rocks and associated petroleum: AAPG Bulletin, **24**, 1529–1547, doi: 10.1306/3d933230-16b1-11d7-8645000102c1865d.

Blatt, H., G. V. Middleton, and R. C. Murray, 1972, Origin of sedimentary rocks: Prentice-Hall Inc., 634.

Blood, R., G. Lash, and L. Bridges, 2013, Biogenic silica in the Devonian shale succession of the Appalachian Basin, USA: Annual Convention and Exhibition, AAPG, Search and Discovery article #50864.

Calvert, S., and T. Pedersen, 1993, Geochemistry of Recent oxic and anoxic marine sediments: Implications for the geological record: Marine Geology, **113**, 67–88, doi: 10.1016/0025-3227(93)90150-t.

Chang, C., M. D. Zoback, and A. Khaksar, 2006, Empirical relations between rock strength and physical properties in sedimentary rocks: Journal of Petroleum Science and Engineering, **51**, 223–237, doi: 10.1016/j.petrol.2006.01.003.

Davis, D., and S. J. Reynold, 1996, Structural geology of rocks and regions, 2nd ed.: Wiley.

Engelder, T., G. G. Lash, and R. S. Uzcátegui, 2009, Joint sets thatenhance production from middle and upper Devonian gasshales of the Appalachian basin: AAPG Bulletin, **93**, 857–889, doi: 10.1306/03230908032.

Flgel, E., 2004, Microfacies of carbonate rocks: Analysis, interpretation and application: Springer Science and Business Media.

Gale, J. F. W., R. M. Reed, and J. Holder, 2007, Natural fractures in the Barnett shale and their importance for hydraulic fracture treatments: AAPG Bulletin, **91**, 603–622, doi: 10.1306/11010606061.

Handin, J., and R. V. Hager, 1957, Experimental deformation of sedimentary rocks under confining pressure: Tests at room temperature on dry samples: AAPG Bulletin, **41**, 1–50, doi: 10.1306/5ceae5fb-16bb-11d7-8645000102c1865d.

Huang, Z., 2018, Partial least squares regression analysis to factor of influence for ecological footprint: Cluster Computing, 1–9.

James, N. P., and B. Jones, 2016, Origin of carbonate sedimentary rocks: John Wiley and Sons, Inc.

Jarvie, D. M., R. J. Hill, T. E. Ruble, and R. M. Pollastro, 2007, Unconventional shale-gas systems: The Mississippian Barnett shale of north-central Texas as one model for thermogenic shale-gas assessment: AAPG Bulletin, **91**, 475–499, doi: 10.1306/12190606068.

Jin, X., S. N. Shah, J.-C. Roegiers, and B. Zhang, 2014, Fracability evaluation in shale reservoirs — An integrated petrophysics and geomechanics approach: Presented at the SPE Hydraulic Fracturing Technology Conference, doi: 10.2118/168589-ms.

Jowett, E. C., 1987, Formation of sulfide-calcite veinlets in the Kupferschiefer Cu-Ag deposits in Poland by natural hydrofracturing during basin subsidence: Journal of Geology, **95**, no. 4, 513–526, doi: 10.1086/629146.

Kias, E., R. Maharidge, and R. Hurt, 2015, Mechanical versus mineralogical brittleness indices across various shale plays: Presented at the SPE Annual Technical Conference and Exhibition, doi: 10.2118/174781-ms.

Kundert, D., and M. Mullen, 2009, Proper evaluation of shale gas reservoirs leads to a more effective hydraulic-fracture stimulation: Rocky Mountain Petroleum Technology Conference, SPE, doi: 10.2118/123586-MS.

Lash, G. G., and D. R. Blood, 2014, Organic matter accumulation, redox, and diagenetic history of the Marcellus formation, southwestern Pennsylvania, Appalachian basin: Marine and Petroleum Geology, **57**, 244–263, doi: 10.1016/j.marpetgeo.2014.06.001.

Lash, G. G., and T. Engelder, 2011, Thickness trends and sequence stratigraphy of the Middle Devonian Marcellus formation, Appalachian basin: Implications for Acadian foreland basin evolution: AAPG Bulletin, **95**, 61–103, doi: 10.1306/06301009150.

Loucks, R. G., R. M. Reed, S. C. Ruppel, and U. Hammes, 2012, Spectrum of pore types and networks in mudrocks and a descriptive classification for matrix-related mudrock pores: AAPG Bulletin, **96**, 1071–1098, doi: 10.1306/08171111061.

Löwemark, L., H.-F. Chen, T.-N. Yang, M. Kylander, E.-F. Yu, Y.-W. Hsu, T.-Q. Lee, S.-R. Song, and S. Jarvis, 2011, Normalizing XRF-scanner data: A cautionary note on the interpretation of high-resolution records from organic-rich lakes: Journal of Asian Earth Sciences, **40**, 1250–1256, doi: 10.1016/j.jseaes.2010.06.002.

Luning, S., and S. Kolonic, 2003, Uranium spectral gamma-ray response as a proxy for organic richness in Black shales: Applicability and limitations: Journal of Petroleum Geology, **26**, 153–174, doi: 10.1111/j.1747-5457.2003.tb00023.x.

Mainali, P., 2011, Chemostratigraphy and the Paleoceanography of the Bossier-Haynesville formation, East Texas basin, TX and LA: M.S. thesis, The University of Texas.

Milad, B., and R. Slatt, 2018, Impact of lithofacies variations and structural changes on natural fracture distributions: Interpretation, **6**, no. 4, T873–T887, doi: 10.1190/INT-2017-0138.1.

Molinares, C. E., R. M. Slatt, and R. Sierra, 2017, The effects of lamination/bedding on the brittleness for the Woodford shale silica-rich intervals, From the Wyche-1 Core-Well Analysis, Pontotoc County, Oklahoma: Presented at the AAPG Annual Convention and Exhibition.

Morford, J. L., and S. Emerson, 1999, The geochemistry of redox sensitive trace metals in sediments: Geochimica et Cosmochimica Acta, **63**, 1735–1750, doi: 10.1016/s0016-7037(99)00126-x.

Neuzil, C. E., and D. W. Pollock, 1983, Erosional unloading and fluid pressures in hydraulically "tight" rocks: Journal of Geology, **91**, no. 2, 179–193, doi: 10.1086/628755.

Olson, J. E., Q. Yuan, J. Holder, and P. Rijken, 2001, Constraining the spatial distribution of fracture networks in naturally fractured reservoirs using fracture mechanics and core measurements: Presented at the SPE Annual Technical Conference and Exhibition, doi: 10.2118/71342-ms.

Pearce, T. H., and I. Jarvis, 1992, Applications of geochemical data to modelling sediment dispersal patterns in distal turbidites: Late quaternary of the Madeira Abyssal plain: SEPM Journal of Sedimentary Research, **62**, 1112–1129, doi: 10.1306/d4267a64-2b26-11d7-8648000102c1865d.

Pearce, T., B. Besly, D. Wray, and D. Wright, 1999, Chemostratigraphy: A method to improve interwell correlation in barren sequences — A case study using onshore Duckmantian/Stephanian sequences (West Midlands, U.K.): Sedimentary Geology, **124**, 197–220, doi: 10.1016/s0037-0738(98)00128-6.

Peng, S., and B. Loucks, 2016, Permeability measurements in mudrocks using gas-expansion methods on plug and crushed-rock samples: Marine and Petroleum Geology, **73**, 299–310, doi: 10.1016/j.marpetgeo.2016.02.025.

Piper, D., and R. Perkins, 2004, A modern vs. Permian black shale — The hydrography, primary productivity, and water-column chemistry of deposition: Chemical Geology, **206**, 177–197, doi: 10.1016/j.chemgeo.2003.12.006.

Price, L. C., 1997, Minimum thermal stability levels and controlling parameters of methane, as determined by C_{15+} hydrocarbon thermal stabilities, *in* T. S. Dyman, D. D. Rice, and P. A. Westcott, eds., Geologic controls of deep natural gas resources in the United States: USGS Bulletin, **2146**, 139–176.

Prothero, D. R., and F. Schwab, 1996, Sedimentary geology: Freeman.

Rickman, R., M. J. Mullen, J. E. Petre, W. V. Grieser, and D. Kundert, 2008, A practical use of shale petrophysics for stimulation design optimization: All shale plays are not clones of the Barnett Shale: Presented at the SPE Annual Technical Conference and Exhibition, doi: 10.2118/115258-ms.

Rijken, P., 2005, Petrographic and chemical controls on subcritical fracture growth: Ph.D. dissertation, University of Texas at Austin.

Rodrigues, N., P. R. Cobbold, H. Loseth, and G. Ruffet, 2009, Widespread bedding-parallel veins of fibrous calcite ('beef') in a mature source rock (Vaca Muerta Formation, Neuquén Basin, Argentina): Evidence for overpressure and horizontal compression: Journal of the Geological Society, **166**, 695–709, doi: 10.1144/0016-76492008-111.

Rothwell, R. G., and F. R. Rack, 2006, New techniques in sediment core analysis: An introduction: Geological Society, London, Special Publications, **267**, 1–29, doi: 10.1144/gsl.sp.2006.267.01.01.

Rowe, H., N. Hughes, and K. Robinson, 2012, The quantification and application of handheld energy-dispersive x-ray fluorescence (ED-XRF) in mudrock chemostratigraphy and geochemistry: Chemical Geology, **324–325**, 122–131, doi: 10.1016/j.chemgeo.2011.12.023.

Sageman, B., and T. Lyons, 2003, Geochemistry of fine-grained sediments and sedimentary rocks: Treatise on Geochemistry, **7**, 115–158, doi: 10.1016/b0-08-043751-6/07157-7.

Sageman, B. B., A. E. Murphy, J. P. Werne, C. A. V. Straeten, D. J. Hollander, and T. W. Lyons, 2003, A tale of shales:

The relative roles of production, decomposition, and dilution in the accumulation of organic-rich strata, middle-upper Devonian, Appalachian basin: Chemical Geology, **195**, 229–273, doi: 10.1016/s0009-2541(02)00397-2.

Slatt, R. M., and Y. Abousleiman, 2011, Merging sequence stratigraphy and geomechanics for unconventional gas shales: The Leading Edge, **30**, 274–282, doi: 10.1190/1.3567258.

Tribovillard, N., T. J. Algeo, T. Lyons, and A. Riboulleau, 2006, Trace metals as paleoredox and paleoproductivity proxies: An update: Chemical Geology, **232**, 12–32, doi: 10.1016/j.chemgeo.2006.02.012.

Verma, S., T. Zhao, K. J. Marfurt, and D. Devegowda, 2016, Estimation of total organic carbon and brittleness volume: Interpretation, **4**, no. 3, T373–T385, doi: 10.1190/int-2015-0166.1.

Wang, F. P., and J. F. W. Gale, 2009, Screening criteria for shale-gas systems: Gulf Coast Association of Geological Societies Transactions, **59**, 779–793.

Wells, F., 2004, A new method to help identify unconventional targets for exploration and development through integrative analysis of clastic rock properties: Houston Geological Society Bulletin, **52**, 34–49.

Young, K. E., C. A. Evans, K. V. Hodges, J. E. Bleacher, and T. G. Graff, 2016, A review of the handheld X-ray fluorescence spectrometer as a tool for field geologic investigations on Earth and in planetary surface exploration: Applied Geochemistry, **72**, 77–87, doi: 10.1016/j.apgeochem.2016.07.003.

Zelt, F. B., 1985, Natural gamma-ray spectrometry, lithofacies, and depositional environments of selected upper Cretaceous marine mudrocks, western United States, including Tropic Shale and Tununk member of Mancos Shale: Ph.D. dissertation, Princeton University.

Zhang, B., T. Zhao, X. Jin, and K. J. Marfurt, 2015, Brittleness evaluation of resource plays by integrating petrophysical and seismic data analysis: Interpretation, **3**, no. 2, T81–T92, doi: 10.1190/int-2014-0144.1.

Keithan G. Martin is a Ph.D. candidate in geology in the Department of Geology and Geography at West Virginia University. He received B.S. and M.S. degrees from Kansas State University. His research focuses on X-ray fluorescence application in reservoir characterization, natural fractures in unconventional systems, and sedimentary geochemistry. He is the corresponding author of this paper.

Liaosha Song is an assistant professor at California State University, Bakersfield. He received a B.S. in geology and an M.S. in marine geology from China University of Petroleum and a Ph.D. in geology from West Virginia University. His research focuses on petrophysics, multiscale image analysis, reservoir characterization, CO_2 sequestration, and pore structure of unconventional reservoirs.

Payam Kavousi is a research assistant professor in the Department of Geology at West Virginia University. He received a Ph.D. in geology from West Virginia University. His current research focuses on fiber-optic application for hydraulic fracturing diagnostics and reservoir monitoring.

Timothy R. Carr is the Marshall Miller professor at West Virginia University and project manager of the Marcellus Energy and Environment Laboratory, and he has worked in various areas of energy geosciences. After graduating from the University of Wisconsin-Madison, he was previously employed at Atlantic Richfield Company, Kansas Geological Survey, and University of Kansas. His current interests include unconventional resources, quantitative techniques, and energy policy.